IEEE Access
Multidisciplinary | Rapid Review | Open Access Journal

Received 21 November 2023, accepted 12 December 2023, date of publication 16 January 2024,
date of current version 25 January 2024.

*Digital Object Identifier 10.1109/ACCESS.2024.3354790*

RESEARCH ARTICLE

# Hardware Supported Fault Detection and Localization Method for AC Microgrids Using Mathematical Morphology with State Observer Algorithm

**FAISAL MUMTAZ[1], KASHIF IMRAN[1], HABIBUR REHMAN[2], (Member, IEEE), AND HAMMAD ALI QURESHI[1]**

[1]U.S. Pakistan Center for Advanced Studies in Energy (USPCAS-E), National University of Sciences and Technology (NUST), Islamabad 44000, Pakistan
[2]Department of Electrical Engineering, American University of Sharjah, Sharjah, United Arab Emirates

Corresponding author: Kashif Imran (kashifimran@uspcase.nust.edu.pk)

This work was supported in part by the Open Access Program from the American University of Sharjah.

**ABSTRACT** Microgrids are the future version of advanced distribution networks due to the fast growth of renewable energy resources near consumers' side. The microgrids are operated in on-grid mode (OGM) with the utility grid, and isolation mode (IM) without the utility grid. This dual operational mode causes protection and control challenges in the microgrids. This research paper suggests an advanced hardware-supported fault detection, phase identification & localization method for AC microgrids. The scheme deploys a Discrete Kalman Filter (DKF) for state estimation of voltage and current signals. Then, a Mathematical Morphology (MM) is engaged for generating a novel fault detection/classification index named segregated energy signature (SES) from estimated voltage and current signals. The system is considered to be faulty if the SES is higher than a predefined threshold setting, while phase identification is achieved by default because of the per-phase implementation of DKF&MM. Moreover, the directional features of the cumulative energy signature (CES) are also computed from MM-based non-fundamental current and voltage to localize the faulty section. The established scheme is tested on the CIGRE microgrid benchmark test bed on Matlab-Simulink software. In addition, the suggested method is also examined on the dSPACE MicroLab testing hardware setup in the Smart grid lab at USPCAS-E, NUST, Pakistan. The result illustrates that the proposed scheme successfully detects, classifies, and localizes the low impedance fault (LIF) as well as high impedance fault (HIF) in both operational modes and topological structures with 96.6% accuracy.

**INDEX TERMS** Distributed generation, discrete Kalman filter, fault detection, hardware in the loop, microgrids protection, mathematical morphology.

## I. INTRODUCTION

Microgrids are self-sufficient networks having various renewable energy-dominated distributed generations (DG), loads, and battery energy storage systems, and are equipped with self-sufficient protection infrastructure [1]. Microgrids are the future grids to provide clean and green energy due to several benefits [2]. However, microgrids face different protection challenges notably i). Fault Detection and Localization [3], ii). Coordination of protection devices [4], iii). Islanding detection [5], [6], iv). High Impedance Faults detection [7], [8], v). Voltage and Frequency Control [9], and vi). Cybersecurity Concerns [10]. Among all the microgrid protection challenges our focus is only designing a protection scheme for detection, classification, and localization of LIF as well as HIF. These challenges are due to the following reasons.

The associate editor coordinating the review of this manuscript and approving it for publication was Arturo Conde.

1. Dynamic levels of current during different operational conditions, the current in OGM of operation is very high while the current during IM of operation is very low.
2. The flow of electric current is bidirectional due to the multiple DGs feeding the grid.
3. A different topological structure like radial, meshed, or loop causes a challenging scenario [11], [12].

Therefore, under such circumstances, the traditional protection strategies exhibit maloperation during harsh system conditions. Hence, we have to design a protection method that is efficient to deal with these operating conditions without any nuisance tripping.

Previous literature addresses microgrid protection issues in many aspects. Different types of protection methods were reported, such as over-current, differential, distance, intelligent, and some modified methods. A novel strategy based on transient wavelet energy was proposed in [13] for the protection of inverter-dominated AC microgrids. The presented scheme was very robust and capable of detecting and localizing different faults under various operating conditions. HIF was detected and classified in microgrids using Kalman filtering [14]. In [15] the authors utilized the wavelet spectrum of energy to identify, classify & localize various faults in AC microgrids during the OGM of operation. Authors in [16] utilized the online current wavelet injection method, traveling waves, and mathematical morphology to protect microgrids from different kinds of faults. Euclidean distance was deployed in [17] to compute superimposed components with waveform similarity for the fault's detection/classification and localization. A Time-time-transform was proposed in [18] for microgrid protection in both the OGM and IM operations. Communication-based microgrid protection scheme was proposed in [7] and [19] through the utilization of high-frequency and impedance respectively. The median filter was utilized as a state estimation algorithm in [5] to extract harmonic features. These harmonic features were then employed to identify, classify, and localize the fault events in the microgrids.

Some intelligent microgrid protection strategies were also reported in the previous literature. Convolution neural network was deployed in [7], and [18] to identify, classify and localize the faulty events in the microgrids. Modal decomposition and combined data mining approach were proposed in [22] to identify, classify, and localize different types of faults in AC microgrids. In [23] empirical mode decomposition was deployed to identify, classify, and localize the faults in the microgrids. A support vector machine was utilized in [24] for the protection of AC microgrids in OGM and IM. A novel protection method based on deep learning was proposed in [25] to protect the microgrid from fault incidents. State observer with the recurrent neural network was suggested in [26] to identify, classify, and localize various faults. A hybrid classifier approach was utilized in [27] for fault location identification in AC microgrids. Artificial intelligence with a traveling wave approach was utilized in [28] to identify, classify, and localize the faults in the microgrids. The authors in [29] utilized a Kalman filter-based approach for protecting the microgrids in both OGM & IM operational conditions under radial, meshed, and loop topologies.

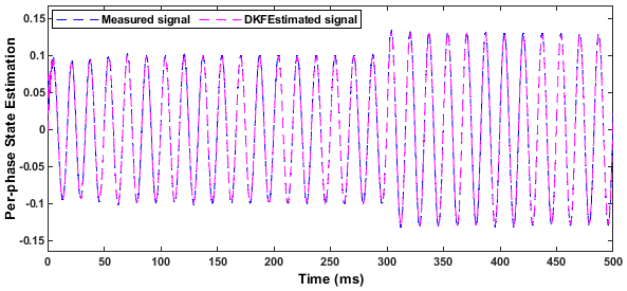


**FIGURE 1.** State-estimation through DKF.

This work suggests a robust hardware-supported fault localization and detection technique for AC microgrids. A DKF was used as a state observer in the proposed scheme to estimate the state of the voltage and current signals. Next, the MM algorithm is engaged to create a novel index called SES, for fault identification and categorization. The system is considered to be faulty if the SES is higher than a predetermined threshold value. To pinpoint the faulty section, parallel computations are also performed on the directional aspects of the CES. On MATLAB/Simulink software, the established scheme is tested on the CIGRE microgrid benchmark. Also, the hardware arrangement based on the dSPACE MicroLab testing environment is used to test the presented method. The results show that the suggested approach successfully locates, classifies, and detects LIF and HIF in both operation modes and topological structures. The value additions of the suggested scheme are as follows.

1. Application of both the DKF and MM in the time and frequency domain for AC microgrid protection.
2. Computationally the proposed algorithms are less intensive.
3. Novel and very simple fault detection/classification and localization indexes are developed.
4. The proposed method deals with noisy measurements as well.
5. The proposed scheme is easy to implement on the hardware setup.
6. The suggested scheme detects both HIFs and LIFs.

The remaining paper organization is as follows. The basic principles of the proposed technique are elaborated in section II. A detailed methodology of the suggested scheme is mentioned in section III. The threshold setting and the utilized CIGRE test benchmark are illustrated in section IV. Section V illustrates the simulation results comprehensively. The Hardware setup and results are explained in section VI. The detailed performance analysis is mentioned in section VII.

**TABLE 1.** Pesudo code of MM algorithm.

| ***The general algorithm for mathematical morphology to extract desired SES and CES from estimated voltage and current signals:*** |
|---|
| ***Step 1.*** Define a structuring element that determines the shape of the operation to be performed on the current and voltage signals. |
| ***Step 2.*** Place the structuring element at each $n^{th}$ sample in the input signals. |
| ***Step 3.*** Perform a comparison between the values of the samples underneath the structuring element and the structuring element itself. |
| ***Step 4.*** Apply the results of the previous operation to the output or result signal at the location corresponding to the center of the structuring element. |
| ***Step 5.*** Slide the SE to the next sample location and repeat *steps 3* and *4* until all samples have been processed. |

At last, the concluding remarks along with future work are provided in section VIII of this paper.

## II. BASIC PRINCIPLE

### A. DKF ALGORITHM

Fault detection in any scheme relies on correct parameter estimation. Therefore, any scheme must choose a parameter estimation algorithm that is capable of estimating electrical parameters with high accuracy. The proposed scheme deployed the DKF, a well-known state estimation algorithm for that purpose. Rudolf E. Kalman, one of its principal theorists, is honored by having the filter retain his name. Figure 1 depicts a detailed illustration of state estimation of per phase voltage signal using the DKF algorithm while a similar estimation is used for voltage as well. In comparison to estimates based just on a single measurement, it generates estimates of unknown variables that are often more accurate. A joint probability distribution across the variables is calculated for each timeframe by the Kalman filtering procedure, commonly known as a linear quadratic estimation. This algorithm is utilized in control theory and statistics [25], [26], [27]. The direction, navigation, and control of moving objects, notably those on land, air, and space, are some technological uses of Kalman filtering. Moreover, Kalman filtering is a time series analysis method that is commonly used in fields like radar and signal processing. Because of these advantages, we deployed DKF for the estimation of per-phase current and voltage signals. The Pseudo code of the DKF algorithm is demonstrated in Table 2.

### B. MM ALGORITHM

A non-linear signal processing tool called MM, created by Matheron and Serra may extract transitory features from

**TABLE 2.** Pseudo code of DKF algorithm.

| ***From the perspective of node 1*** |
|---|
| ***Initialization: t= 0;*** |
| Initialize the state estimate $x$ and state covariance $P$ |
| Initialize the process noise covariance matrix $Q$ |
| Initialize the observation noise covariance matrix $R$ |
| ***Prediction:*** |
| Predict the next state estimate ***x_pred*** using the transition model: $x\_pred = F * x + B * u$ where $F$ is the state transition matrix, $B$ is the input matrix, and $u$ is the control input. |
| Predict the state covariance ***P_pred*** using the process model: $P\_pred = F * P * F' + Q$ where $F'$ is the transpose of $F$ |
| ***Update:*** |
| Compute the innovation or measurement residual $y$: $y = z - H * x\_pred$ where $z$ is the observed measurement and $H$ is the observation matrix |
| Compute the innovation or measurement covariance S: $S = H * P\_pred * H' + R$ where $H'$ is the transpose of $H$ |
| ***Compute the Kalman gain K:*** $K = P\_pred * H' * inv(S)$ where $inv(S)$ is the inverse of $S$ |
| Update the state estimate $x$: $x = x\_pred + K * y$ |
| Update the state covariance $P$: $P = (I - K * H) * P\_pred$ where $I$ is the identity matrix |
| Repeat the prediction and update steps for each time step or observation until the end of the time series. |
| ***until t < tend*** |

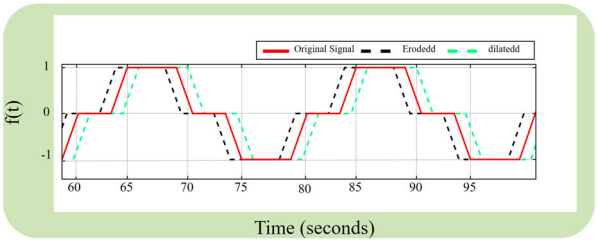


**FIGURE 2.** Mathematical morphological signature depiction.

processing current & voltage signals. MM is a time-domain signal processing technique that, in contrast to STFT and WT, involves only simple computations (like maxima, and minima) and whose correctness never depends on the periodicity of the signal. As opposed to the STFT and WT, which may deform the signal, a more significant feature of the MM is its ability to extract the ascending or descending edges from

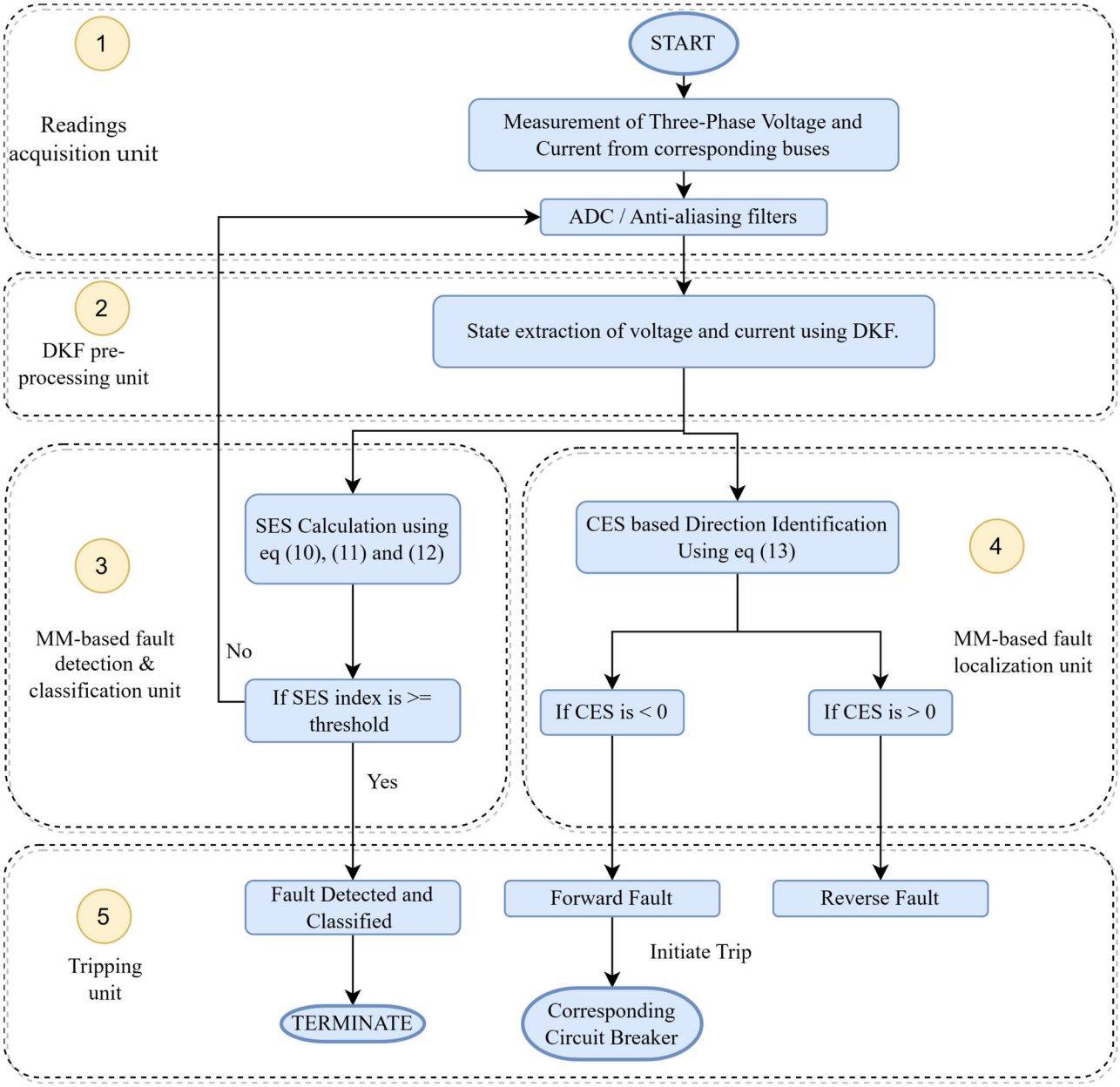


**FIGURE 3.** Flow chart of proposed hardware supported scheme.

a processing signal more visibly [16]. Despite that structuring elements (SE) are fundamental to all MM-based tasks, including dilatation, erosion, opening, and closing as depicted in Figure 2. The detailed computational steps of the MM algorithm are shown in Table 1. When performing any type of MM-based operation, SE slides over the processing signal like a window to extract transitory features that resemble its structure [32]. Hence, for applications in power systems, the best SE should be chosen. The SE for the electrical signal is as follows.

$$Y_{\text{dil}} = \max_{0\le n-m\le n} \{f(n-m) + g(m)\} \tag{1}$$

$$Y_{\text{ero}} = \min_{0\le n+m\le n} \{f(n+m) + g(m)\} \tag{2}$$

Here $Y_{dil}$ and $Y_{ero}$ represent dilated and eroded signals respectively. Furthermore, $f$ is a signal to be dilated or eroded, whereas $g$ is SE.

$$Y_{open} = (fog_n) \tag{3}$$

$$Y_{close} = (f.g_n) \tag{4}$$

Opening and closing operations of "$f$" by "$g$" denoted by "$fog$" and "$f \cdot g$" respectively.

## III. PROPOSED METHOD

The proposed protection method designed for the microgrid encompasses five operational units; readings acquisition, DKF pre-processing unit, MM-based fault detection/

classification unit, MM-based fault localization unit, and at last the tripping unit. The flow diagram of the suggested method is illustrated in Figure 3.

### A. READINGS ACQUISITION UNIT

The voltage/current readings acquired from the faulty bus were pre-processed through the Butterworth filter for antialiasing purposes. Secondly, these measurements are analog signatures, and our protection relay and the DKF algorithm need discrete values. Therefore, the analog-to-digital conversion is done through the ADC module of the reading acquisition unit. The discrete version of both current and voltage signals is defined by eqs (5) and (6) respectively.

$$I_r = I \sin(\omega t + \varphi) \tag{5}$$

$$V_r = V \sin(\omega t + \varphi) \tag{6}$$

where $I_r$ is the measured current and $V_r$ is the measured voltage of the corresponding faulty bus. $I$ is the current magnitude while $V$ is the voltage magnitude. However, $\omega$ and $\varphi$ are angular frequency and measurement noise respectively. At the next step, the converted discrete current/voltage signals are sent to DKF for the exact state estimation because the measured readings are noisy and are not suited for direct fault index calculation.

### B. DKF PRE-PROCESSING UNIT

The discrete voltage & current signals received from the previous stage are provided to DKF for the estimation of electrical magnitudes. It is noted that the DKF is implemented in a per-phase manner therefore, only a related mathematical depiction is presented in the whole manuscript to avoid complexity. The remaining three phases are simply 120° degrees apart. The state-space model.

$$X_{n+1} = Bx_n + W \tag{7}$$

$$i_n = Yx_n + u_n \tag{8}$$

The tuned parameters of DKF utilized in this study are defined by Equations 9.

$$x_n \text{ system states; } \hat{X}_n = \begin{bmatrix} I_n & I_{n-1} \end{bmatrix}^{-1}; b = \begin{bmatrix} 1 & 0 \end{bmatrix}^T;$$
$$H = \begin{bmatrix} 1 & 0 \end{bmatrix}^T; \quad A = \begin{bmatrix} 2\cos\omega_0 & -1 \\ 1 & 0 \end{bmatrix} \tag{9}$$

The Table 2 algorithm works using this state space model and tuning parameters to generate desired estimates of current and voltage signals. The trigonometric derivatives of eqs (5) and (6) are taken for the acquisition of an iterative conversion of the obtained signals as follows.

$$\widehat{I_{e+1}} = 2I_n + \emptyset \tag{10}$$

$$\widehat{V_{e+1}} = 2V_n + \emptyset \tag{11}$$

The estimated current and voltage signatures obtained through DKF operation are given by equations (12) and (13).

$$\widehat{I_e} = I_n + \emptyset \tag{12}$$

$$\widehat{V_e} = V_n + \emptyset \tag{13}$$

Where, $I_e$ is the estimated current and $V_e$ is the estimated voltage from the corresponding faulty bus. $I_n$ is the magnitude of the estimated current while $V_n$ is the magnitude of the estimated voltage. However, $\emptyset$ depicts the random error or white Gaussian noise. These estimated voltage and current signals are provided to a mathematical morphological algorithm for the calculation of fault detection and classification index and also for fault localization indexing.

### C. MM-BASED FAULT DETECTION & CLASSIFICATION UNIT

The MM is engaged in this unit for the calculation of fault detection & classification index. The estimated voltage & current of each phase are provided at the input of MM in a segregated manner to compute per-phase SES. The SES is computed as follows.

$$SES_a = \widehat{I_e} * \widehat{V_e} \tag{14}$$

$$SES_b = \widehat{I_e} * \widehat{V_e} \tag{15}$$

$$SES_c = \widehat{I_e} * \widehat{V_e} \tag{16}$$

If the value of SES of any single/multiple phases is above the threshold of the relevant phase, the phase is regarded as faulty. As the index is computed in phase segregated manner, no separate fault classification unit is needed. Moreover, this unit sends two signals one of them is the OR-based fault detected (OBFD) signal which is sent to the main protection unit of the relay while the second is per phase fault detection (PPFD) signal provided to the corresponding phase circuit breaker's tripping unit.

### D. MM-BASED FAULT LOCALIZATION UNIT

This section mainly focuses on two parts: i. direction identification using CES, and ii- communication-based main & backup facility. Initially, the calculation of CES should be done then a detailed description of communication-based main & backup be provided.

The faulty section is identified in the presented scheme using the directional trends of the CES. The CES is simply calculated by the mathematical sum of eqs (14), (15), and (16). The computed CES is as follows.

$$CES = SES_a + SES_a + SES_a \tag{17}$$

It is noted that the CES is negative during forward faults while positive during reverse faults. Therefore, the negative direction of CES in any section indicates the presence of forward faults.

Secondly, as we can observe in the microgrid after the occurrence of a fault the CES is negative on several buses. Therefore, it is difficult to decide faulty section based on just this direction signal. Based on this main reason the proposed scheme utilized the communication infrastructure of the microgrid to communicate with three adjacent relays to take the correct decision. The detailed depiction of this scenario is illustrated in Figure 4. It is the first three-bus test system on which the whole proposed scheme is implemented. It comprises two zones; i- Zone 1 and ii- Zone 2, the

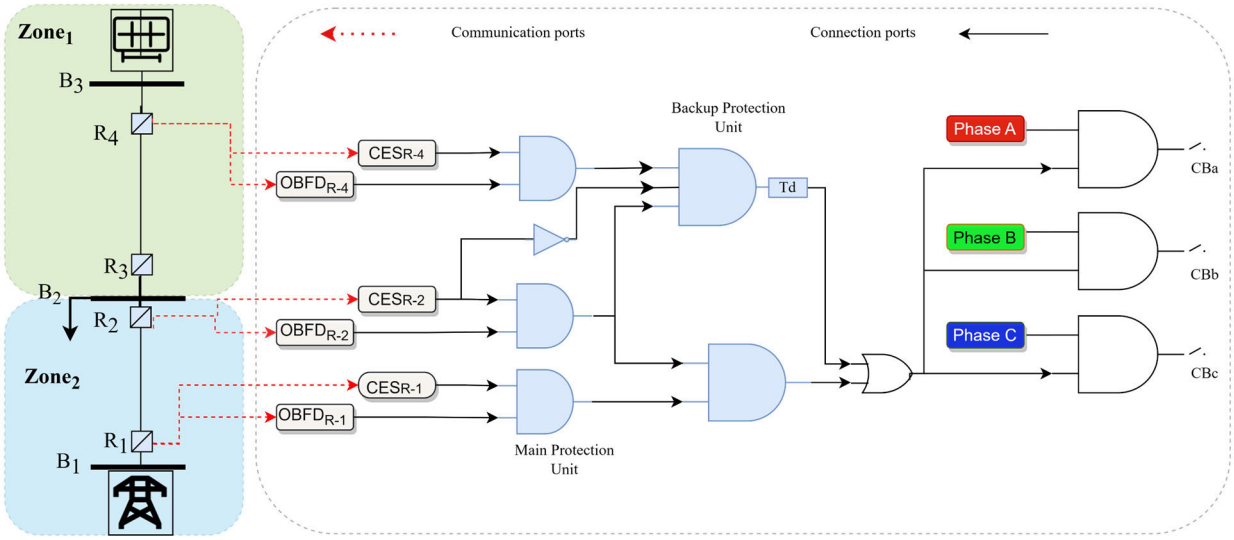


**FIGURE 4.** Initial 3-bus test bed for implementation of MM based fault localization logic.

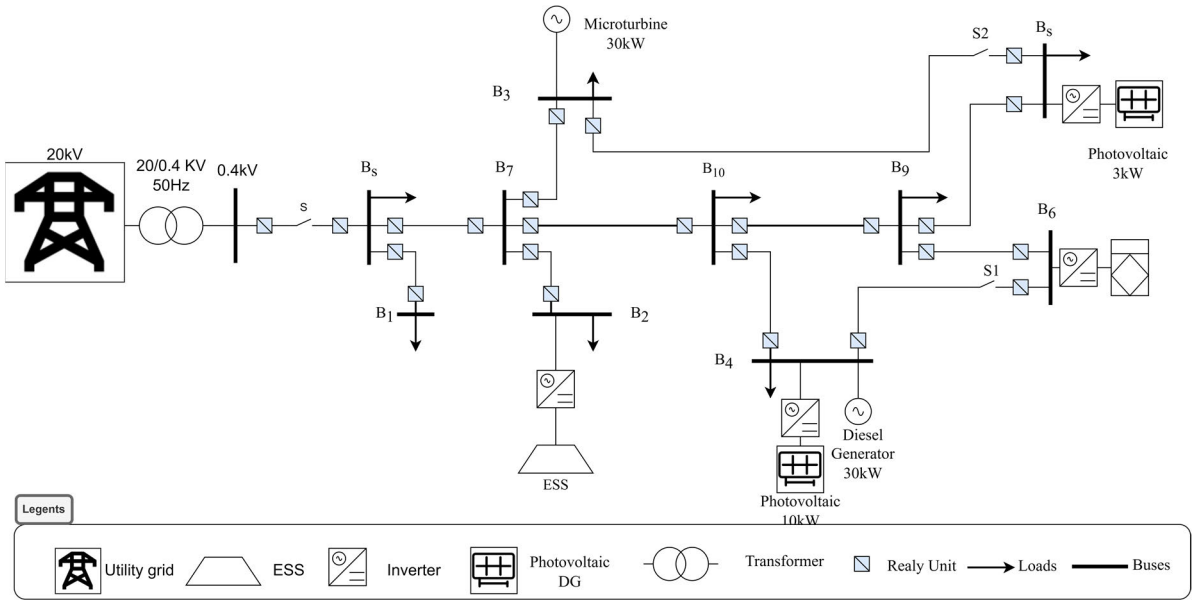


**FIGURE 5.** CIGRE benchmark test bed for AC microgrid.

relay-1 (R-1) is considered a reference relay to understand the concept of a communication-assisted MM-based fault localization unit.

The R-1 is communicated to R-2 and R-4 through the communication link, every relay sends and receives two signals from the other relay units: i- OBFD and, ii- CES direction signal. The following logic is followed for the main and backup unit's operation.

$$\textit{Main unit operation} \begin{Bmatrix} \textit{if} \;\; \textit{CES is negative at R1} \\ \& \;\; \textit{CES is negative at R2} \end{Bmatrix} \tag{18}$$

$$\textit{however} \begin{Bmatrix} \textit{if} \;\; \textit{CES is negative at R1} \\ \& \;\; \textit{CES is positive at R2} \end{Bmatrix} \tag{19}$$

Then, the directional trends on R-4 signals are cross-checked

$$\textit{Secondry unit operation} \begin{Bmatrix} \textit{if} \;\; \textit{CES is negative at R1} \\ \& \;\; \textit{CES is negative at R4} \end{Bmatrix} \tag{20}$$

Finally, the OR operation is performed at the output of the main and backup protection units. However, it is noted that there is an intentional delay of 3 ms to operate the main protection first. Then the trip signal (TS) is sent to the tripping unit.

### E. TRIPPING UNIT

The tripping unit receives two signals from previous stages one of them is PPFD and the second one is TS. They are

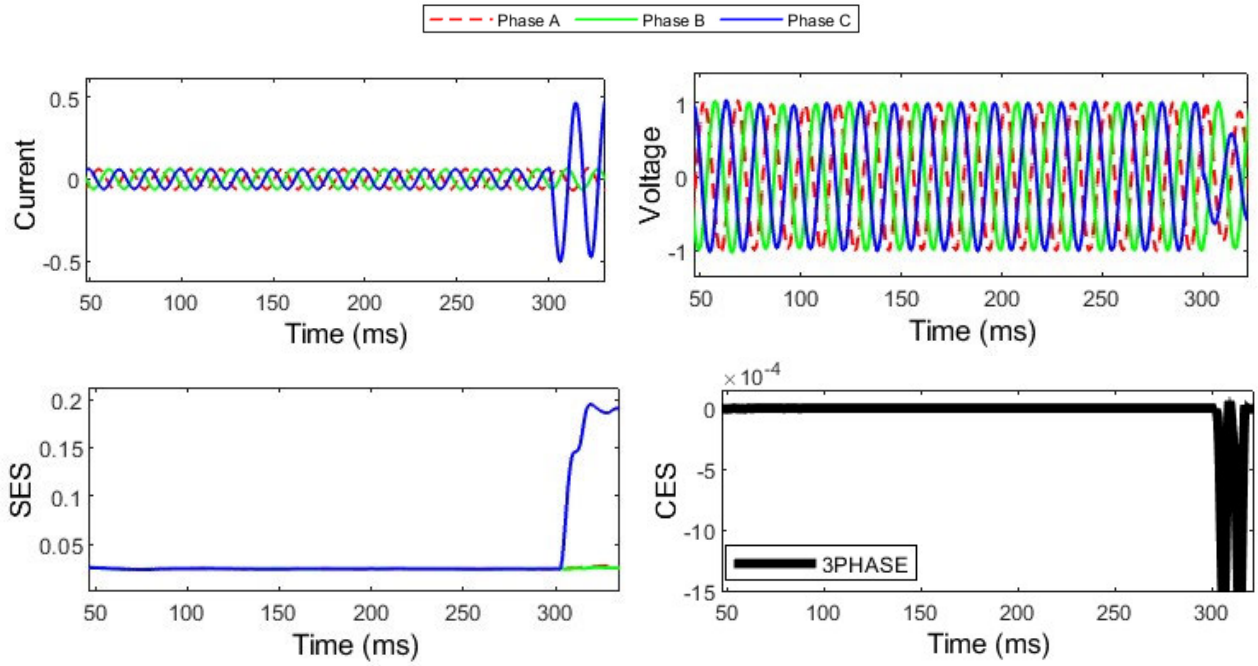


**FIGURE 6.** A single phase to ground fault in islanded operational mode when switch-1 is open.

processed through AND-gate. If both of them are triggered the corresponding CB gets operated on to protect the healthy system.

$$Tripping\ the\ CB \left\{ \begin{array}{ll} if & \text{PPFD} = 1 \\ \& & \text{TS} = 1 \end{array} \right\} \tag{21}$$

## IV. CIGRE BENCHMARK TEST BED & PRE-DEFINED THRESHOLD

This subsection mainly focuses on the AC microgrid network that is engaged in the proposed scheme for fault analysis. Secondly, the threshold settings are explained in the scheme.

### A. CIGRE BENCHMARK TEST BED

The proposed scheme utilized a well-renowned CIGRE benchmark test system for extensive fault analysis. The single-line diagram of the CIGRE benchmark test network is illustrated in Figure 5. The test system comprises 3 inverter-based DGs, 2 synchronous-based DGs, and one battery energy storage system. It consists of 10 buses and the utility grid is connected to the rest of the microgrid via a point of common coupling. The circuit breaker (CB), CB-S is utilized in the proposed test system to switch the operation mode between OGM and IM. The test system had 9-line sections, while switches S-1 and S-2 were provided for the topology changing purpose. The detailed parameterization of the CIGRE benchmark test system is acquired from [14].

### B. PRE-DEFINED THRESHOLD

Threshold settings are very important in any scheme for rapid fault detection/classification and localization. Hence, the suggested scheme was tested in different worst-case scenarios and operating conditions for the exact calculation of the threshold. It is observed that ideally, the SES is 0 during normal operating conditions while more than zero during the faulty situation. Therefore, to cover all kinds of faults in the real-time practical environment the SES threshold is chosen to be 0.05. If the SES is higher than this pre-defined threshold value, the system is in a fault condition. Secondly, the CES is negative for forward faults, while positive for reverse faults.

## V. SIMULATION RESULTS

The section described the fault analysis of the suggested method in different operating modes, topology resistances, locations, and different DG's intermittencies. Almost all kinds of phase-to-phase and phase-to-ground faults were tested to validate the performance of the suggested method. The faults were also checked during the LIF and the HIF in addition the single-phase tripping was also checked.

### A. SINGLE-PHASE TRIPPING

Single-phase tripping is very important in any scheme to detach only the faulty phase from the healthy network. Therefore, numerous single-phase faults were tested in the proposed scheme for validation, while only one of the cases is presented here due to lack of space. A fault at a single-phase C occurred on the line section between bus 3 and bus 7 at a time stamp of 300 msec. It is seen from Figure 6 that the presented method efficiently detects and classifies the fault immediately. The negative direction of the Cumulative energy signature at the corresponding relay illustrates the presence of a forward fault in this section. Therefore, the

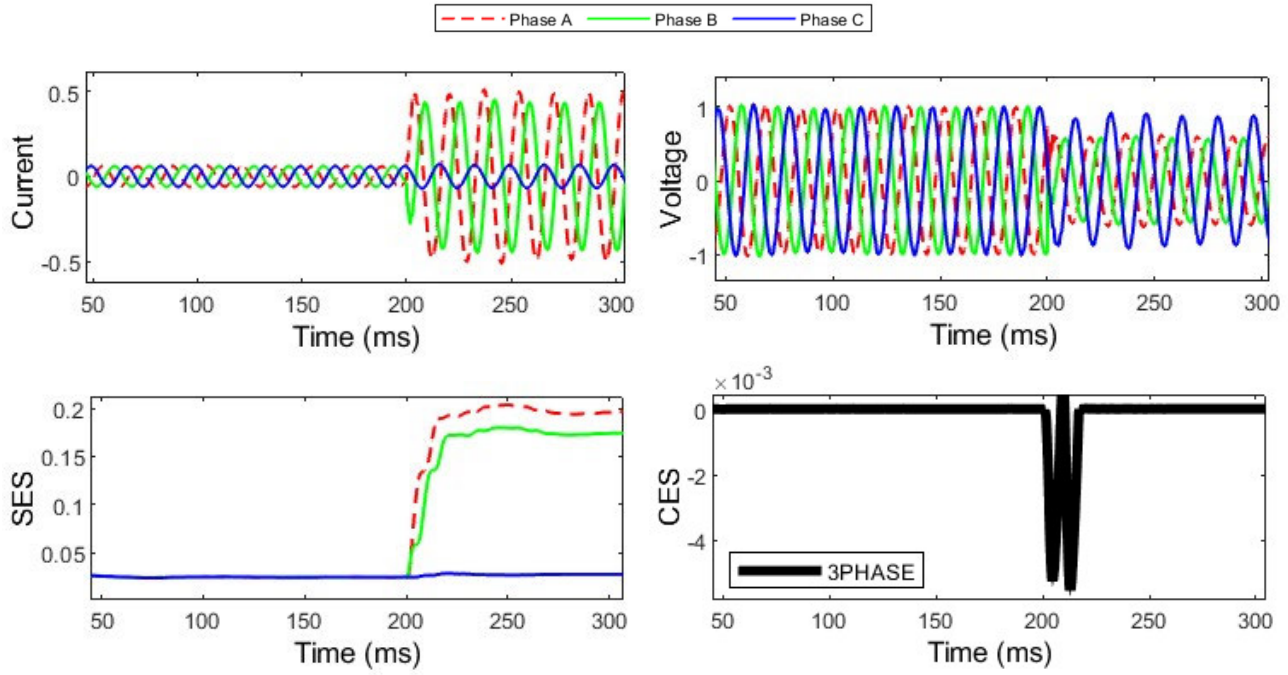


**FIGURE 7.** A double phase to ground HIF in OGM operational mode when switch-1 and switch-2 are open.

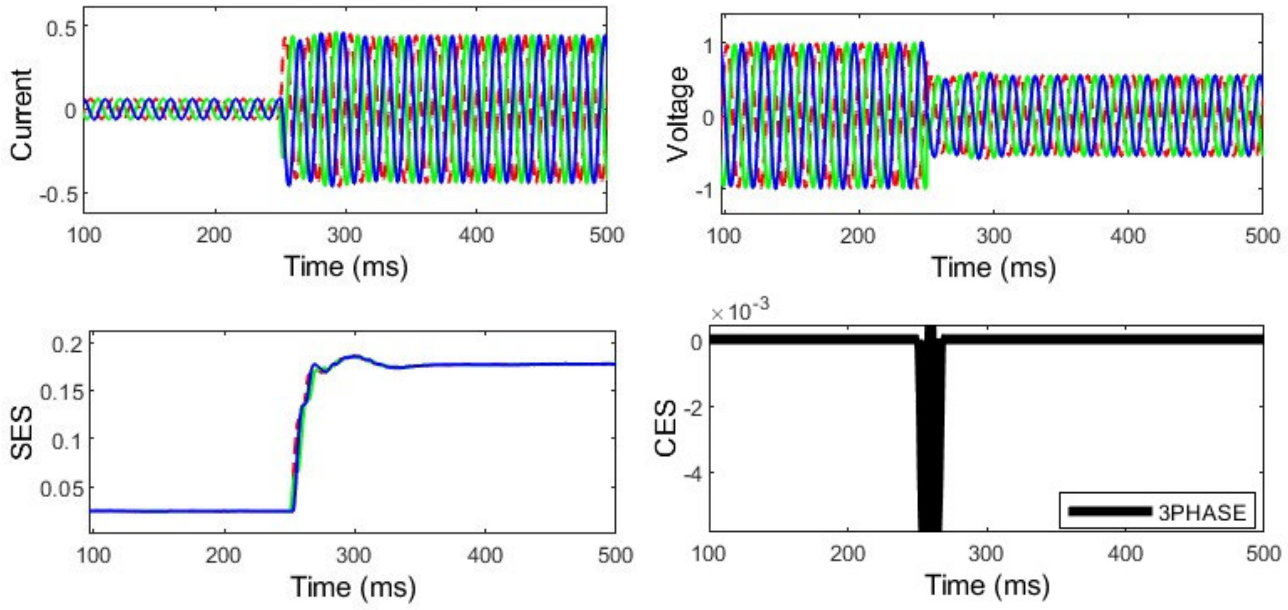


**FIGURE 8.** A three phase to ground fault in islanded operational mode when switch-2 is open.

main protection unit of the relevant relay of this line section successfully locates the fault. The tripping signals of some other single-phase fault cases are depicted in Figure 11(a).

### B. HIGH IMPEDANCE RESULTS

Detection of HIF is very challenging due to a very low fault current [10]. Many high-impedance fault cases are performed to authenticate the capability of the suggested method. A double-phase BA-G fault occurred at the line section between bus 4 and bus 10 of the CIGRE test system at a time stamp of 200 msec. It is seen from Figure 7 that the presented method successfully detected and classified the fault immediately. The negative direction of the CES at the related relay illustrates the existence of a forward fault in

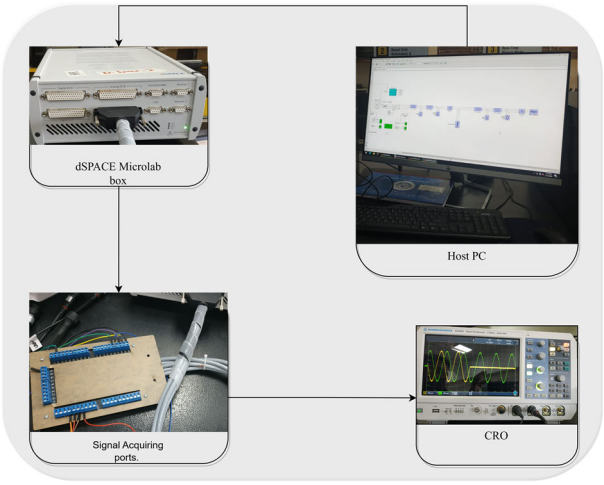


**FIGURE 9.** Hardware supported experimental setup.

this section. Therefore, the main protection unit of the related relay of this line section successfully locates the fault. The tripping signals of some double line-to-ground HIF cases are depicted in Figure 11(b).

### C. THREE PHASE FAULTS

Three-phase faults are the most threatening faults while less occurring in power systems. Therefore, the effectiveness of the presented method was also authenticated in three-phase faults under different operation conditions and microgrid topologies. A three-phase ABC-G fault occurred at the line section between bus 9 and bus 10 of the CIGRE test system at the time stamp of 250 msec. It is seen from Figure 8 that the suggested scheme effectively detected and classified the fault immediately. The negative direction of the CES at the corresponding relay illustrates the existence of a forward fault in this section. Therefore, the main protection unit of the relevant relay of this line section successfully located the fault. The tripping signals of some 3-phase cases are illustrated in Figure 11(c). A case of a no-fault scenario is also shown in Figure 11(d).

## VI. HARDWARE IN THE LOOP RESULTS

The presented microgrid protection scheme is also tested on hardware in the loop setup using the Dspace micro-lab box in the smart grid lab at USPCAS-E, NUST, Pakistan.

A detailed illustration of the experimental setup developed for hardware validation is shown in Figure 9. The experimental setup has been created by using a host PC that is used as a Controlled desk, is attached to the Dspace micro-lab box, and the analog outputs of the Dspace micro-lab box are connected to the cathode ray's oscilloscope. Different kinds of fault conditions are tested on hardware setup to validate the proposed scheme.

A case study of single-phase tripping is depicted in Figure 10. In this, a real-time CRO signature of the voltage signal was acquired at a faulty bus during a single-phase fault.

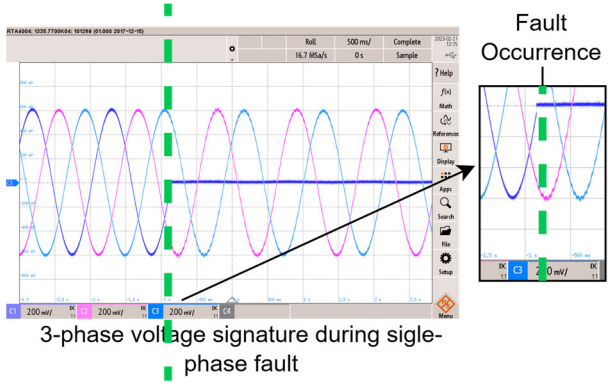


**FIGURE 10.** Hardware results of proposed scheme.

It indicates that the single-phase fault initiated from the dotted green line and the voltage of the faulty phase is facing a sag.

The proposed fault detection method can be implemented in dSPACE MicroLab hardware as follow.

1. By connecting the necessary sensors to the hardware channels.
2. Acquiring the measured voltage and current data.
3. Preprocessing the data to remove noise.
4. Extracting the relevant features from the preprocessed data.
5. Generation of fault detection indexes of proposed algorithm using these features.
6. Validating and testing the algorithm with simulated or real fault data.
7. Integrating the algorithm into the control or monitoring system, and continuously monitoring the system using the hardware's visualization tools.
8. This implementation allows for real-time monitoring and detection of faults in the system.

## VII. PERFORMANCE DEPICTION

The performance of the proposed method was validated through testing across various fault types, including phase-to-phase and phase-to-ground faults. Additionally, the method's effectiveness was evaluated in both LIF and HIF, with examination also conducted on single-phase tripping scenarios.

The presented microgrid protection scheme is compared with some previous methods to check the performance of the proposed scheme as depicted in Table 3. The chosen methods contain some signal processing-based schemes and some intelligent methods. Three types of performance indicators under observation are as follows: i. computational burden, ii. Accuracy, and iii. Internal operation time of the schemes.

### A. COMPUTATIONAL BURDEN ANALYSIS

Computational burden analysis is vital in evaluating the performance of microgrid protection schemes, especially concerning their implementation feasibility. Comparing a proposed scheme's computational burden against existing methods helps in determining its efficiency and practicality. There are different parameters for computational burden

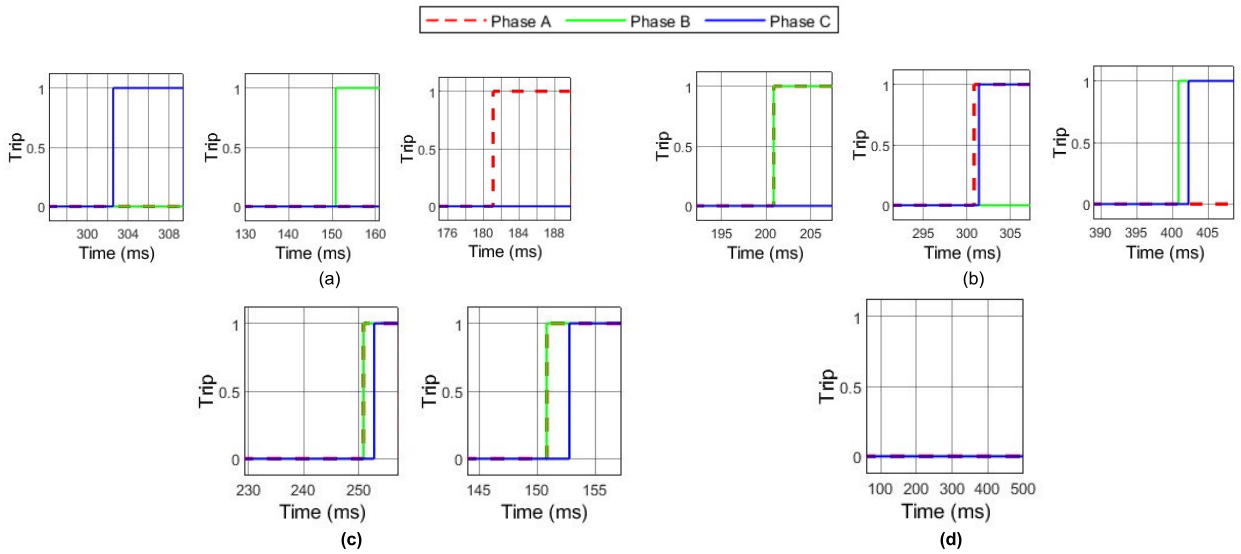


**FIGURE 11.** (a) Tripping singnature of some single line to ground fault in different operational mode. (b) Tripping singnature of some Double line to ground fault in different operational mode. (c) Tripping singnature of some Three phase faults in different operational mode. (d) No fault condition.

**TABLE 3.** Performance analysis of proposed method with some existing counter parts.

| Comparison Parameters | Compared benchmark Methods | | | | Proposed method |
|---|---|---|---|---|---|
| | Harmonic content-based method [5] | State observer-based method [26] | Kalman filter-based method [29] | CNN-based method [20] | |
| Computational burden | Very low | High | Low | High | Very low |
| Accuracy | 98% | 99% | 90% | 99% | 96.6% |
| Internal operating time | 5msec | 6 msec | 18ms | 50ms | <15 ms |
| Operation Modes | Both modes | Both modes | Both modes | Both modes | Both modes |
| Topologies | Radial Looped meshed | Radial Looped meshed | Radial Looped meshed | Radial Looped | Radial Looped meshed |
| Noise Consideration | Yes | Yes | Yes | No | Yes |
| Ease of Implementation | Very easy | Difficult | Easy | Difficult | Very easy |
| Hardware Implementation | No | No | No | No | Yes |

analysis of any proposed scheme while we check the processing time of the proposed algorithm for computational burden analysis. The computational burden of the proposed scheme is cross-checked with some existing methods as depicted in Table 3. It is observed that the proposed approach is computationally less demanding than some of the existing methods.

### B. ACCURACY ANALYSIS

The proposed scheme is very accurate and reliable for the protection of microgrids as depicted in Table 3. Approximately 30 different types of faults are tested in various microgrid operational regimes, out of which 29 cases were successfully detected. Hence, the proposed scheme is 96.6% accurate. The accuracy of the proposed scheme is computed as follows.

$$Accuracy = \frac{number\ of\ sucessfull\ operations}{total\ number\ of\ operations} \quad (22)$$

### C. INTERNAL OPERATION TIME ANALYSIS

The proposed scheme successfully detected the fault in less than 15 milliseconds in almost all cases. Therefore, by comparison, it is observed that this detection time is much less than most of the existing methods. Moreover, some other parameters like operational modes, topologies, noise consideration, ease of implementation, and hardware implementation have also been compared to check the efficacy of the proposed scheme. The proposed scheme shows better performance as compared to some of the existing benchmarked methods. However, the proposed scheme also lacks some existing compared methods in a few aspects as mentioned in Table 3.

## VIII. CONCLUSION

This paper proposed a robust hardware-based fault localization method for AC microgrids. Initially, the state estimation of voltage and current signals was done through DKF. Then,

the MM was used to develop the SES, a new fault identification and categorization index. The system is regarded as faulty if the SES exceeds a certain threshold value, and phase-segregated DKF& MM implementation is done for the autonomous classification of faults. To locate the faulty section, the directional properties of the CES were computed concurrently. On MATLAB/Simulink software, the established scheme was tested in the CIGRE microgrid benchmark. Also, the hardware setup based on the dSPACE MicroLab testing environment is used to validate the presented scheme. The results indicate that all types of faults are successfully detected by the proposed scheme in $<$15 msec with 96.6% accuracy and with a very low computational burden.

## ACKNOWLEDGMENT

This article represents the opinions of the author(s) and does not mean to represent the position or opinions of the American University of Sharjah. This research utilized hardware in the Smart Grid Laboratory, USPCAS-E, National University of Sciences and Technology.

## REFERENCES

[1] A. Cagnano, E. De Tuglie, and P. Mancarella, "MicroGrids: Overview and guidelines for practical implementations and operation," *Appl. Energy*, vol. 258, Jan. 2020, Art. no. 114039, doi: 10.1016/j.apenergy.2019.114039.

[2] N. Hussain, M. Nasir, J. C. Vasquez, and J. M. Guerrero, "Recent developments and challenges on AC microgrids fault detection and protection systems—A review," *Energies*, vol. 13, no. 9, p. 2149, May 2020, doi: 10.3390/en13092149.

[3] H. R. Baghaee, D. Mlakic, S. Nikolovski, and T. Dragicevic, "Support vector machine-based islanding and grid fault detection in active distribution networks," *IEEE J. Emerg. Sel. Topics Power Electron.*, vol. 8, no. 3, pp. 2385–2403, Sep. 2020, doi: 10.1109/JESTPE.2019.2916621.

[4] R. Tiwari, R. K. Singh, and N. K. Choudhary, "Coordination of dual setting overcurrent relays in microgrid with optimally determined relay characteristics for dual operating modes," *Protection Control Modern Power Syst.*, vol. 7, no. 1, pp. 1–12, Dec. 2022, doi: 10.1186/s41601-022-00226-1.

[5] F. Mumtaz, K. Imran, A. Abusorrah, and S. B. A. Bukhari, "Harmonic content-based protection method for microgrids via 1-dimensional recursive median filtering algorithm," *Sustainability*, vol. 15, no. 1, p. 164, Dec. 2022, doi: 10.3390/su15010164.

[6] F. Mumtaz, K. Imran, A. Abusorrah, and S. B. A. Bukhari, "An extensive overview of islanding detection strategies of active distributed generations in sustainable microgrids," *Sustainability*, vol. 15, no. 5, p. 4456, Mar. 01, 2023, doi: 10.3390/su15054456.

[7] S. Beheshtaein, R. Cuzner, M. Savaghebi, S. Golestan, and J. M. Guerrero, "Fault location in microgrids: A communication-based high-frequency impedance approach," *IET Gener., Transmiss. Distrib.*, vol. 13, no. 8, pp. 1229–1237, Apr. 2019.

[8] M. Manohar, E. Koley, and S. Ghosh, "Microgrid protection against high impedance faults with robustness to harmonic intrusion and weather intermittency," *IET Renew. Power Gener.*, vol. 15, no. 11, pp. 2325–2339, Aug. 2021, doi: 10.1049/rpg2.12167.

[9] S. M. Malik, X. Ai, Y. Sun, C. Zhengqi, and Z. Shupeng, "Voltage and frequency control strategies of hybrid AC/DC microgrid: A review," *IET Gener., Transmiss. Distrib.*, vol. 11, no. 2, pp. 303–313, Jan. 26, 2017, doi: 10.1049/iet-gtd.2016.0791.

[10] F. Nejabatkhah, Y. W. Li, H. Liang, and R. Reza Ahrabi, "Cyber-security of smart microgrids: A survey," *Energies*, vol. 14, no. 1, p. 27, Dec. 01, 2020, doi: 10.3390/en14010027.

[11] B. Mahamedi and J. E. Fletcher, "Trends in the protection of inverter-based microgrids," *IET Gener., Transmiss. Distrib.*, vol. 13, no. 20, pp. 4511–4522, Oct. 22, 2019, doi: 10.1049/iet-gtd.2019.0808.

[12] A. A. Memon and K. Kauhaniemi, "A critical review of AC microgrid protection issues and available solutions," *Electr. Power Syst. Res.*, vol. 129, pp. 23–31, Dec. 03, 2015, doi: 10.1016/j.epsr.2015.07.006.

[13] D. Liu, A. Dysko, Q. Hong, D. Tzelepis, and C. D. Booth, "Transient wavelet energy-based protection scheme for inverter-dominated microgrid," *IEEE Trans. Smart Grid*, vol. 13, no. 4, pp. 2533–2546, Jul. 2022, doi: 10.1109/TSG.2022.3163669.

[14] F. Mumtaz et al., "High impedance faults detection and classification in renewable energy-based distribution networks using time-varying Kalman filtering technique" *Eng. Proc.*, vol. 20, no. 1, p. 34, 2022, doi: 10.3390/engproc2022020034.

[15] X. Zheng, Y. Zeng, M. Zhao, and B. Venkatesh, "Early identification and location of short-circuit fault in grid-connected AC microgrid," *IEEE Trans. Smart Grid*, vol. 12, no. 4, pp. 2869–2878, Jul. 2021, doi: 10.1109/TSG.2021.3066803.

[16] M. Dodangeh and N. Ghaffarzadeh, "Fault detection, location, and classification method on compressed air energy storages based inter-connected micro-grid clusters using traveling-waves, current injection method, online wavelet, and mathematical morphology," *Int. Trans. Electr. Energy Syst.*, vol. 31, no. 12, Dec. 2021, doi: 10.1002/2050-7038.13190.

[17] M. A. Jarrahi, H. Samet, and T. Ghanbari, "Protection framework for microgrids with inverter-based DGs: A superimposed component and waveform similarity-based fault detection and classification scheme," *IET Gener., Transmiss. Distrib.*, vol. 16, no. 11, pp. 2242–2264, Jun. 2022, doi: 10.1049/gtd2.12438.

[18] O. A. Gashteroodkhani, M. Majidi, M. S. Fadali, M. Etezadi-Amoli, and E. Maali-Amiri, "A protection scheme for microgrids using time-time matrix z-score vector," *Int. J. Electr. Power Energy Syst.*, vol. 110, pp. 400–410, Sep. 2019, doi: 10.1016/j.ijepes.2019.03.040.

[19] R. Bhargav, C. P. Gupta, and B. R. Bhalja, "Unified impedance-based relaying scheme for the protection of hybrid AC/DC microgrid," *IEEE Trans. Smart Grid*, vol. 13, no. 2, pp. 913–927, Mar. 2022, doi: 10.1109/TSG.2021.3129532.

[20] S. B. A. Bukhari, C. Kim, K. K. Mehmood, R. Haider, and M. Saeed Uz Zaman, "Convolutional neural network-based intelligent protection strategy for microgrids," *IET Gener., Transmiss. Distrib.*, vol. 14, no. 7, pp. 1177–1185, Apr. 2020, doi: 10.1049/iet-gtd.2018.7049.

[21] M. Manohar, E. Koley, S. Ghosh, D. K. Mohanta, and R. C. Bansal, "Spatio-temporal information based protection scheme for PV integrated microgrid under solar irradiance intermittency using deep convolutional neural network," *Int. J. Electr. Power Energy Syst.*, vol. 116, Mar. 2020, Art. no. 105576, doi: 10.1016/j.ijepes.2019.105576.

[22] S. Jamali and S. Ranjbar, "Phase selective protection in microgrids using combined data mining and modal decomposition method," *Int. J. Electr. Power Energy Syst.*, vol. 128, Jun. 2021, Art. no. 106727, doi: 10.1016/j.ijepes.2020.106727.

[23] M. Biswal, C. Durga Prasad, P. Ray, and N. Kishor, "Modified complete ensemble empirical mode decomposition based HIF detection approach for microgrid system," *Int. J. Electr. Power Energy Syst.*, vol. 141, Oct. 2022, Art. no. 108254, doi: 10.1016/j.ijepes.2022.108254.

[24] A. Srivastava and S. K. Parida, "A robust fault detection and location prediction module using support vector machine and Gaussian process regression for AC microgrid," *IEEE Trans. Ind. Appl.*, vol. 58, no. 1, pp. 930–939, Jan. 2022, doi: 10.1109/TIA.2021.3129982.

[25] J. Hu, Z. Liu, J. Chen, W. Hu, Z. Zhang, and Z. Chen, "A novel deep learning–based fault diagnosis algorithm for preventing protection malfunction," *Int. J. Electr. Power Energy Syst.*, vol. 144, Jan. 2023, Art. no. 108622, doi: 10.1016/j.ijepes.2022.108622.

[26] F. Mumtaz, H. H. Khan, A. Zafar, M. U. Ali, and K. Imran, "A state-observer-based protection scheme for AC microgrids with recurrent neural network assistance," *Energies*, vol. 15, no. 22, p. 8512, Nov. 2022, doi: 10.3390/en15228512.

[27] S. Jamali, A. Bahmanyar, and S. Ranjbar, "Hybrid classifier for fault location in active distribution networks," *Protection Control Mod. Power Syst.*, vol. 5, no. 1, Dec. 2020, doi: 10.1186/s41601-020-00162-y.

[28] D. A. Etingov, P. Zhang, Z. Tang, and Y. Zhou, "AI-enabled traveling wave protection for microgrids," *Electr. Power Syst. Res.*, vol. 210, Sep. 2022, Art. no. 108078, doi: 10.1016/j.epsr.2022.108078.

[29] F. Mumtaz, K. Imran, S. B. A. Bukhari, K. K. Mehmood, A. Abusorrah, M. A. Shah, and S. A. A. Kazmi, "A Kalman filter-based protection strategy for microgrids," *IEEE Access*, vol. 10, pp. 73243–73256, 2022, doi: 10.1109/ACCESS.2022.3190078.

[30] W. Zhou and J. Hou, "A new adaptive robust unscented Kalman filter for improving the accuracy of target tracking," *IEEE Access*, vol. 7, pp. 77476–77489, 2019, doi: 10.1109/ACCESS.2019.2921794.
[31] J. Qi, K. Sun, J. Wang, and H. Liu, "Dynamic state estimation for multi-machine power system by unscented Kalman filter with enhanced numerical stability," *IEEE Trans. Smart Grid*, vol. 9, no. 2, pp. 1184–1196, Mar. 2018, doi: 10.1109/TSG.2016.2580584.
[32] M. A. Shah, S. B. A. Bukhari, K. Imran, K. K. Mehmood, F. Mumtaz, A. Abusorrah, S. A. A. Kazmi, and A. Wadood, "High speed protection of medium voltage DC distribution system using modified mathematical morphology," *IET Renew. Power Gener.*, vol. 16, no. 14, pp. 3134–3148, Oct. 2022, doi: 10.1049/rpg2.12564.

**FAISAL MUMTAZ** received the B.S. degree in electrical engineering power from the University of Wah, Pakistan, in 2015, and the M.S. degree in electrical engineering power from the U.S. Pakistan Center for Advanced Studies in Energy, National University of Sciences and Technology (NUST), Islamabad, Pakistan, in 2021, where he is currently pursuing the Ph.D. degree. From 2017 to 2018, he was an Instructor with the Department of Electrical Engineering, Swedish Institute of Science and Technology. His research interests include machine learning, microgrid protection, state estimation, distributed generation, discrete signal processing, and system identification. He received the USAID fully-funded scholarship for the master's degree.

**KASHIF IMRAN** received the B.Sc. and M.Sc. degrees in electrical engineering from the University of Engineering and Technology, Lahore (UET Lahore), in 2006 and 2008, respectively, and the Ph.D. degree in electrical engineering from the University of Strathclyde, in 2015. From 2006 to 2007, he was with the Transmission and Distribution Division, SIEMENS, and the Power Distribution Design Section, NESPAK. He was a Faculty Member of UET Lahore and COMSATS University Lahore. From 2018 to 2021, he was the Inaugural Head of the Department of Electrical Power Engineering, U.S. Pakistan Center for Advanced Studies in Energy (USPCSC-E), National University of Sciences and Technology (NUST), Islamabad, where he is currently an Associate Professor. His primary research interests include energy policy, optimization for power systems and electricity markets operations and planning, and power system protection. He received the Commonwealth Scholarship for the Ph.D. degree.

**HABIBUR REHMAN** (Member, IEEE) received the B.Sc. degree in electrical engineering from the University of Engineering and Technology, Lahore (UET Lahore), Pakistan, in 1990, and the M.S. and Ph.D. degrees in electrical engineering from The Ohio State University, Columbus, OH, USA, in 1995 and 2001, respectively. He has wide experience in the areas of power electronics, motor drives, and power systems in both industry and academia. From 1998 to 1999, he was a Design Engineer with Ecostar Electric Drive Systems and Ford Research Laboratory, where he was a member of the Electric, Hybrid, and Fuel Cell Vehicle Development Programs. From 2001 to 2006, he was with the Department of Electrical Engineering, United Arab Emirates University, Al Ain, United Arab Emirates, as an Assistant Professor. In 2006, he joined the Department of Electrical Engineering, American University of Sharjah, where he is currently a Professor. His primary research interests include power electronics and their application to power systems, adjustable-speed drives, and alternative energy vehicles.

**HAMMAD ALI QURESHI** received the B.S. degree in electrical engineering from Air University, Islamabad, in 2019. He is currently pursuing the M.S. degree in electrical power engineering from the National University of Sciences and Technology (NUST), Islamabad, Pakistan. His research interests include electric vehicle chargers and the integration of renewable energy into electric vehicle charging stations.